Decomposing thermal fluctuations with hydrodynamic modes

Xiaohui Deng,[1] Xiaoyu Wei,[2] Xiaoping Wang,[2] and Ping Sheng[1,*]

[1]*Department of Physics, Hong Kong University of Science and Technology, Clear Water Bay, Kowloon, Hong Kong, China*

[2]*Department of Mathematics, Hong Kong University of Science and Technology, Clear Water Bay, Kowloon, Hong Kong, China*

(Received 6 December 2019; accepted 29 May 2020; published 22 June 2020)

We have obtained analytically the complete set of hydrodynamic modes (HMs) for a two-dimensional (2D) fluid confined within a channel with the Navier slip boundary condition at the hydrodynamic boundary. The HMs are orthogonal to each other and hence each represents an independent degree of freedom. We show that the HMs can be used to recursively generate a time series of random thermal fluctuations of displacement velocity, with identical statistical distributions as those obtained from MD simulations. By projecting the HMs onto molecular dynamics (MD) configurations and evaluating the resulting decay time from the autocorrelation function, we obtain from MD the eigenvalues of the HMs. Multiplying two different HMs and integrating as a function of z from center of the channel towards the fluid-solid interface, the position of the hydrodynamic boundary (HDB) is unambiguously identified as the point at which the integral vanishes. Invariably the HDB is located inside the fluid domain and not on the liquid-solid interface. With the knowledge of the HDB position, the value of the slip length can be obtained directly from HM's dispersion relation. We show that in terms of the complete set of HMs, the fluctuation-dissipation theorem may be expressed in a simple expression involving the average of the inverse of the eigenvalues. Besides offering an alternative perspective on thermal fluctuations and hydrodynamic boundary, the present work opens the possibility of using modulated boundary conditions to manipulate thermal fluctuations in mesoscopic channels, which can lead to interesting statistical mechanical consequences.

DOI: 10.1103/PhysRevE.101.063104

I. INTRODUCTION

Thermal fluctuations in fluid are usually manifest as localized tiny displacement velocity variations [1,2], or as self-diffusion of the fluid molecules. It is an inherent part of the physical phenomena associated with thermal equilibrium that is the foundation of statistical mechanics. In the past few decades, the advent of nano- and microfluidics has focused attention on the effect of fluid-solid interfaces on confined fluids [3–7]. In an earlier work [8] it was shown that by considering the low-order continuum hydrodynamic modes in a 2D channel, one can identify the location and characteristics of the hydrodynamic boundary (HB), with excellent agreement with the results of molecular dynamics (MD) simulations. Interestingly, the HB is always located inside the fluid domain. In this work we report the analytical solution for the complete set of hydrodynamic modes in a 2D channel. With this solution set one can easily obtain a time series of velocity fluctuations that is statistically identical to that obtained by molecular dynamics (MD). Besides confirming the earlier results [8] on the location and characteristics of the hydrodynamic boundary, we have also obtained a simple expression for the fluctuation-dissipation theorem (FDT) in terms of hydrodynamic modes' eigenvalues. Since the boundary condition is an inherent part of the hydrodynamic modes, the present work opens the possibility of manipulating thermal fluctuations in mesoscopic channels via boundary condition modulations, with the attendant statistical mechanical consequences.

In what follows, we present the analytical solution of the 2D hydrodynamic modes in Sec. II. This is followed by a description of our approach in Sec. III in which MD simulations [9,10] are used to obtain the eigenvalues of the HMs, with the subsequent determination of the HB position and the relevant slip length. In Sec. IV the setup of the MD simulations, the use of projection of HM onto the MD configurations to obtain the autocorrelation function, and the evaluation of the diffusion constant, are detailed. In Sec. V we give a brief description on the generation of a fluctuating velocity displacement time series that exhibits identical statistical properties as that obtained by MD. In Sec. VI we illustrate the approach used to identify the location of the hydrodynamic boundary as well as the value of the slip length. Derivation of the FDT [10,11] in terms of the hydrodynamic modes is given in Sec. VII, with comparison to the MD simulation result on the diffusion constant. We conclude in Sec. VIII with a short recapitulation and an outlook for future works.

II. HYDRODYNAMIC MODES

According to the kinetic theory of fluids [4,12], thermal fluctuations arise from the thermal motion of molecules. In the continuum limit, a fruitful approach to study the motions of an infinite number of interacting molecules is to use the continuum equation of motion [1] and view the thermal fluctuations as the actuation of the hydrodynamic modes via the equipartition theorem. For the 2D liquid system, the hydrodynamic modes are the eigenfunctions of the incompressible

*sheng@ust.hk

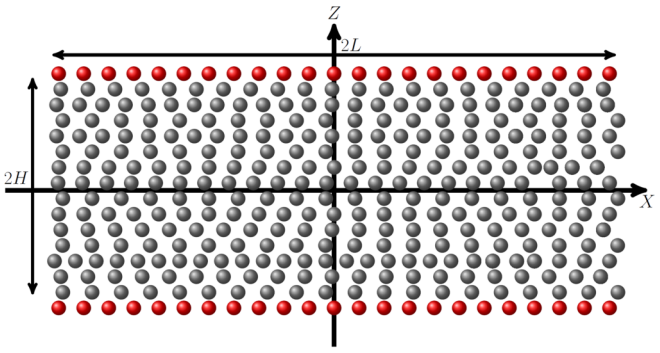

(a)

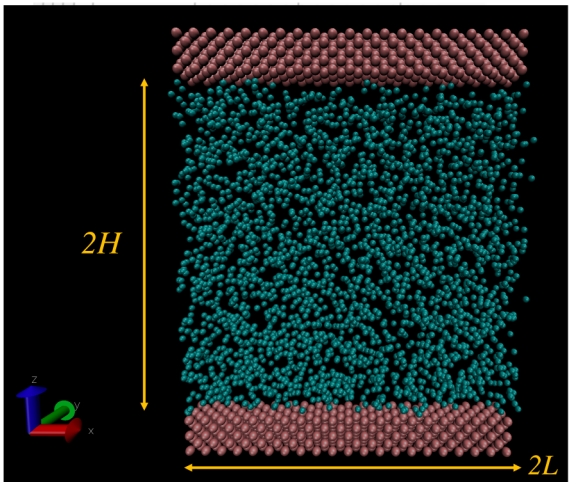

(b)

FIG. 1. (a) A schematic representation of a fluid confined within a mesoscopic 2D channel of length $2L$ and height $2H$. Gray solid balls denote fluid atoms and red solid balls denote wall atoms, here only one layer is shown. (b) A snapshot of our MD simulation configuration.

Navier–Stokes equation characterized by the mass density ρ, velocity field $\vec{v}(\vec{x})$, and viscosity η:

$$\rho\frac{\partial\vec{v}(\vec{x},t)}{\partial t} = -\nabla p + \eta\nabla^2\vec{v}(\vec{x},t), \quad \nabla\cdot\vec{v}(\vec{x},t) = 0, \tag{1}$$

where p denotes pressure, t is the time, and we have neglected the nonlinear term $\rho\vec{v}\cdot(\nabla\vec{v})$ since we will not be considering high velocity flows. To solve for the hydrodynamic modes, we first take the curl on both sides of Eq. (1) to obtain an equation for the vorticity $\vec{\Omega}$:

$$R\frac{\partial\vec{\Omega}(\vec{x},t)}{\partial t} = \nabla^2\vec{\Omega}(\vec{x},t), \quad \vec{\Omega} = \nabla\times\vec{v}, \tag{2a}$$

$$\nabla^2\vec{\Omega}(\vec{x},t) = -\lambda R\vec{\Omega}(\vec{x},t), \tag{2b}$$

where $R = \rho/\eta$. Equation (2b) is in the form of an eigenvalue equation, in which the eigenvalue λ characterizes the time dependence of $\vec{\Omega}\sim\exp(-\lambda t)$. In what follows, we consider the geometry of a 2D channel with width $2H$ along the z direction as shown schematically in Fig. 1(a), with the center of the channel designated as $z = 0$ and the direction along the channel axis denoted as the x direction. A snapshot of the molecular dynamics simulation of the sytem is shown in Fig. 1(b). Since we would like to consider the hydrodynamic modes in the absence of any external force acting on the system, hence from Newton's law only those solutions with stationary center of mass will be taken into account.

As the velocity has only x and z components, it follows that $\vec{\Omega} = (\partial v_z/\partial x - \partial v_x/\partial z)\hat{j}$ has only a y component and therefore may be regarded as a scalar quantity. We denote it as $\Omega(\vec{x},t)$. By writing $\Omega(\vec{x},t) = \exp(-\lambda t)\Omega(\vec{x})$ in anticipation of exponentially decaying solutions, we obtain from Eq. (2) the following solution form [13]:

$$\Omega(x,z) = \Gamma\sin(k_z z+\alpha)\cos(k_x x), \tag{3}$$

Where Γ denotes the amplitude of the mode, and $k_x^2 + k_z^2 = \lambda R$. Here Γ,α are arbitrary constants to be determined by the additional conditions imposed on the solution. From the definition of the vorticity function and the incompressibility condition $\partial v_x/\partial x + \partial v_z/\partial z = 0$, we can eliminate v_x by differentiating Ω [Eq. (3)] with respect to x and note that $-\partial v_x/\partial z\partial x = -\partial_z(\partial v_x/\partial x) = -\partial_z(-\partial v_z/\partial z) = +\partial^2 v_z/\partial z^2$, so that

$$\frac{\partial^2 v_z}{\partial x^2} + \frac{\partial^2 v_z}{\partial z^2} = -\Gamma k_x\sin(k_z z+\alpha)\sin(k_x x). \tag{4}$$

Here v_z is subject to the boundary condition that $v_z = 0$ at the hydrodynamic boundary. Similarly, for v_x one obtains

$$\frac{\partial^2 v_x}{\partial x^2} + \frac{\partial^2 v_x}{\partial z^2} = -\Gamma k_z\cos(k_z z+\alpha)\cos(k_x x), \tag{5}$$

where v_x is specified to satisfy the Navier boundary condition [14]: $\mp l_s(\partial v_x/\partial z) = v_x$ at the hydrodynamic boundary, where l_s denotes the slip length [3]. It should be noted that owing to the liquid structure in the vicinity of solid-liquid interface, the hydrodynamic boundary cannot be at the liquid-solid molecular interface. Instead, it is located at $y = \pm h = \pm(H-\Delta)$, where Δ is the distance of the hydrodynamic boundary from the molecular interface $y = \pm H$ [8]. More on the determination of the hydrodynamic boundary will be noted below.

There are two sets of solutions: the set that displays antisymmetry with respect to $z = 0$, and the set that displays symmetry with respect to $z = 0$. Below we first consider the antisymmetric solution set.

A. Antisymmetric solutions

Antisymmetric solutions of Eqs. (4) and (5) that satisfy all the boundary conditions plus the incompressibility and stationary center of mass conditions can be written as

$$v_x = \Gamma\left[\Lambda\sinh(k_x z) + \frac{k_z}{\lambda R}\cos(k_z z+\alpha)\right]\cos(k_x x), \tag{6a}$$

$$v_z = \Gamma\left[\Lambda\cosh(k_x z) + \frac{k_x}{\lambda R}\sin(k_z z+\alpha)\right]\sin(k_x x), \tag{6b}$$

where the parameter Λ is determined by the condition

$$\Lambda\cosh(k_x h) = -\frac{k_x}{\lambda R}\cos(k_z h)\sin\alpha, \quad \alpha = \frac{\pi}{2},\frac{3\pi}{2},\frac{5\pi}{2},-- \tag{6c}$$

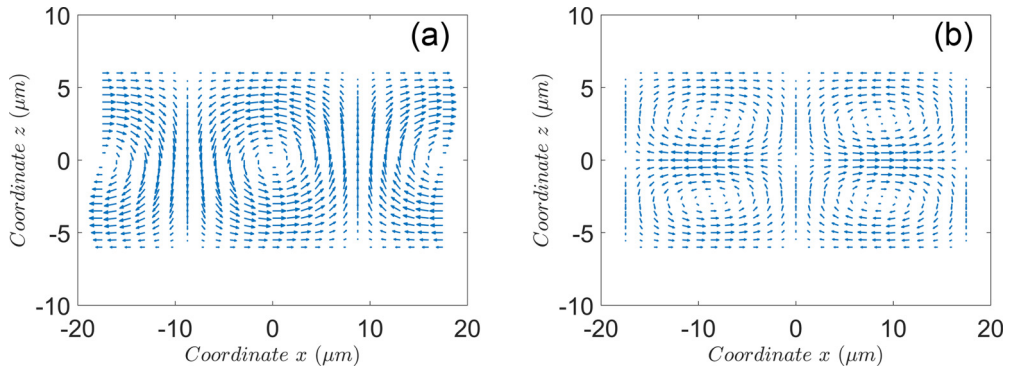

FIG. 2. (a) A plot of the velocity field for a particular antisymmetric hydrodynamic eigenmode with $k_x = \pi/L$. Here we choose $L = 17.48$ μm and $H = 6$ μm. Net flow in one periodic unit is zero. (b) A plot of the velocity field for a particular symmetric hydrodynamic eigenmode with $k_x = \pi/L$. Here we choose the same sample size $L = 17.48$ μm and $H = 6$ μm. The net flow in one periodic unit is zero, consistent with the zero volume force. Unlike the antisymmetric modes, there does not exist centers of vortices at $z = 0$. There can be a $k_x = 0$ antisymmetric mode, but not for the symmetric case.

and the dispersion relation is given by

$$\lambda R l_s + k_x \tanh(k_x h) + k_z \tan(k_z h) = 0, \tag{6d}$$

in conjunction with the constraint $k_x^2 + k_z^2 = \lambda R$.

The validity of the solution can be checked by substituting the solutions into the differential equation with the relevant boundary conditions, as well as the incompressibility and the stationary center of mass conditions. For example, the incompressibility condition can be easily verified by differentiating Eq. (6a) by x and Eq. (6b) by z, and adding the results. That $v_z = 0$ at the hydrodynamic boundary can be verified by combining (6b) and (6c), setting $z = \pm h$, and recognizing that $\cos(\pm k_z h)\sin\alpha = \sin(\alpha \pm k_z h)$ for $\alpha = \pi/2, 3\pi/2$, etc., since $\cos\alpha = 0$. To verify the Navier boundary condition at $z = -h$, simply solve for Λ in Eq. (6c) and substitute the result into (6a) at $z = -h$. That would yield (with $\alpha = \pi/2$ for simplicity) $v_x|_{z=-h} = -\Gamma l_s \cos(k_z h)$, where relation (6d) has been used. By differentiating Eq. (6a), setting $z = -h$, and using Eq. (6c), we obtain $\partial_z v_x|_{z=-h} = -\Gamma\cos(k_z h)$. It follows that $\partial_z v_x|_{z=-h} = v_x|_{z=-h}/l_s$, the desired result.

The antisymmetric hydrodynamic modes have the character of vortex and antivortex pairs. This is illustrated in Fig. 2(a) for a particular mode with a nonzero k_x.

B. Symmetric solutions

For the solution set symmetric with respect to $z = 0$, the procedure is similar. By following the same variable separation procedure as described above (except there cannot be a $k_x = 0$ mode as in the antisymmetric case owing to the stationary center of mass condition) we can get the relevant expressions as

$$v_x = \Gamma\left[\Lambda\cosh(k_x z) + \frac{k_z}{\lambda R}\cos(k_z z)\right]\cos(k_x x), \tag{7a}$$

$$v_z = \Gamma\left[\Lambda\sinh(k_x z) + \frac{k_x}{\lambda R}\sin(k_z z)\right]\sin(k_x x), \tag{7b}$$

$$\Lambda\sinh(k_x h) = -\frac{k_x}{\lambda R}\sin(k_z h), \tag{7c}$$

with the dispersion relation given by

$$\lambda R l_s + k_x \coth(k_x h) - k_z \cot(k_z h) = 0. \tag{7d}$$

The parameters in the above equations must be solved together with the constraint $k_x^2 + k_z^2 = \lambda R$. The symmetric hydrodynamic modes also display the characteristic feature of vortex and antivortex pairs. A typical example is illustrated in Fig. 2(b).

C. Equipartition and the mode amplitude

Since the hydrodynamic eigenmodes are the eigenfunctions of the Laplacian operator, they are orthogonal to each other and hence each represents an independent degree of freedom. It follows that the amplitude Γ_β of the solution is determined by the equipartition theorem [1], i.e., each hydrodynamic mode should have $(1/2)k_B T$ of thermal kinetic energy:

$$\frac{1}{2}\rho\Gamma_\beta^2\int\left[v_{\beta,x}^2(x,z) + v_{\beta,z}^2(x,z)\right]dxdz = \frac{1}{2}k_B T, \tag{8a}$$

$$\Gamma_\beta^2 = \frac{k_B T}{\rho\int\left[v_{\beta,x}^2(x,z) + v_{\beta,z}^2(x,z)\right]dxdz}. \tag{8b}$$

Here we use subscript β for the eigenfunction index. Hence $v_{\beta,x}$ means the x component of the βth velocity eigenfunction. Similarly for the z component.

For a system with an infinite spatial domain, the amplitude is necessarily infinitesimal. However, for a given spatial location, the incoherent addition of an infinite number of modes would still give rise to a finite fluctuation amplitude.

D. Completeness of the solutions

It is important to note that the symmetric solutions, combined with the antisymmetric solutions, satisfy the following completeness condition:

$$\sum_\beta \vec{v}_\beta(\vec{r})\vec{v}_\beta(\vec{r}') = \delta(\vec{r} - \vec{r}')\int|\vec{v}_\beta(\vec{r})|^2 d\vec{r}, \tag{9}$$

where $\vec{r} = (x, z)$. Proof of the completeness condition is presented in Appendix A [13].

E. Evaluation of eigenvalues and eigenfunctions

In Secs. II A and II B above we have presented two types of eigenfunctions and their corresponding dispersion relations. Here we illustrate the solution procedure for the eigenfunctions and eigenvalues from the two dispersion relations.

Antisymmetric and symmetric modes have the same solution procedures. Here we use the antisymmetric modes to illustrate the solution procedure. In Eq. (6d), h, l_s, and R are the given system parameters and k_x is the sequenced input wave vector which characterizes the periodicity along the x direction. Once all four parameters are given, we can solve for the unknown k_z under the constraint $k_x^2 + k_z^2 = \lambda R$. For a given k_x, k_z has infinite number of solutions due to the periodic property of $\tan(x)$. By substituting pairs of k_x and k_z back to (6a) and (6b) one can explicitly obtain the eigenfunctions, while the eigenvalues can be obtained from the relation $\lambda = (k_x^2 + k_z^2)/R$.

When the channel's length L is given, wave vector k_x can be any value selected from $\{k_x = m_x\pi/L | m_x \in \mathrm{N}\}$. For each specified m_x, an infinite number of k_z indexed by $m_z \in \mathrm{N}^+$ can generate either antisymmetric or symmetric solutions. Therefore we can label the eigenwave vector $\vec{k} = (k_x, k_z)$ by using the 2-tuple (m_x, m_z). Since the 2-tuple is countable, we rearrange the eigenvalues in a sequence by using one (integer) index β to label the ordering in accordance to the magnitude of λ from small to large (decay time from large to small). In this fashion we map the eigenvalues from the 2-tuple to its natural ordering λ_β. Such a label will become useful as shown below, for ordering the decay times of the HMs.

From the above, we see that the eigenfunctions and eigenvalues can be labeled either by (k_x, k_z) or by β.

III. OUTLINE OF THE STRATEGY IN USING MD TO DETERMINE THE HMs' EIGENVALUES

What we have presented above is basically the analytical form of the HMs in which h and l_s are treated as given system parameters, from which k_z and λ can be derived. However, in MD simulations h and l_s are implicit parameters, not known *a priori*. Therefore we intend, in the subsequent sections, to use MD in conjunction with the form of the HM with k_z *being treated as a variable, to first identify the eigenvalues of the HMs*. The system parameters h and l_s are subsequently obtained by using the orthogonality property of the HMs. In other words, the solution steps are in the reverse order as that described in Sec. II E above. While the technical steps of this process are detailed in the subsequent sections; here we give an overview of the approach so as to anticipate the later developments.

The basic principle of this approach is that even though in MD there is no explicit delineation of a "hydrodynamic boundary," yet the fact that it exists implicitly in MD simulations cannot be in doubt. Hence if continuum hydrodynamics is correct, then the HM with the correct value of k_z (i.e., that which gives the eigenvalue), once projected onto the MD configuration and followed in its time evolution, should exhibit a local maximum in the decay time in its self-correlation. This is guaranteed by the variational derivation of the Navier boundary condition from the principle of minimum dissipation [15,16]. As evidenced below, this fact is indeed true.

Once the eigenvalues (and hence the eigenfunctions) are determined, we multiply two different HMs and integrate the product from $z = 0$, i.e., the center of the channel, towards the channel boundary. Since the HMs are the eigenfunctions of symmetric matrices, they are orthogonal to each other and hence the integral must vanish at the HB. By using this process the position of the HB, i.e., the value of h, can be unambiguously identified and with overdetermination, since the integral should vanish for the product of any two different HMs.

The determination of the HB position also carries with it the value of the slip length, since once h, k_x, k_z (and therefore λ) are known, the slip length can be obtained from the dispersion relation, Eq. (6d) or (7d). This manner of determining the slip length is noted to be very different from the usual MD approach [7,9,17–21]. The present approach has the advantage of knowing the reference point, i.e., the hydrodynamic boundary, from which the slip length should be measured. This is especially important since the slip length is usually fairly small in magnitude and hence the precise position of the reference point is crucial for determining its value.

IV. MOLECULAR DYNAMICS SIMULATIONS

A. Parameter settings

Molecular dynamics (MD) simulation of Lennard-Jones (LJ) potential fluid [22] confined between two parallel solid walls were carried out to numerically verify the results from the perspective of continuum hydrodynamic modes [9,10].

There are two types of atoms in our MD system: fluid atoms and solid wall atoms. Solid wall has three atomic layers arranged in a face-centered-cubic lattice, with each atom constrained to move within a harmonic potential centered on the lattice site. The force constant for the solid atoms is given by $k_0 = 900$ in default MD unit of our system, with the harmonic potential given by $U = \frac{1}{2}k_0|\Delta\vec{r}|^2$, where $\Delta\vec{r}$ denotes the deviation vector from the equilibrium position of the solid atom. The value of the force constant was chosen to ensure that the mean-square displacement of the wall atoms does not exceed 10% of the nearest-neighbor distance, in accordance with the Lindemann criterion [23]. Interaction between the solid atoms was removed. Detailed settings can be found in Ref. [8]. Periodic boundary conditions were applied along all three directions, with the y periodicity being very short so as to suppress low energy excitations.

The interactions between the fluid atoms and that between the solid and fluid atoms are both described by the LJ potential, where *i,j* refer to the atomic type. Here "solid" is denoted by subscript w and "fluid" by subscript f; σ is LJ potential's atomic size parameter and ε denotes the interaction energy unit. In addition, we use m to denote the atomic mass. We set $\varepsilon_{wf} = 1.16\varepsilon$, $\sigma_{wf} = 1.04\sigma$, $\delta_{wf} = 0.7$ and $\varepsilon_{ff} = 1.16\varepsilon$, $\sigma_{ff} = 1.04\sigma$, and $\delta_{ff} = 1$. The average number density of the fluid is set at $\rho = 0.805/\sigma^3$, and the fluid system is kept at equilibrium state under a constant temperature $3.5\varepsilon/k_B$. To keep our MD system at constant temperature rather than

constant energy, Nose-Hoover chains [24] algorithm with chain length $l_c = 2$ was used as the thermostat. Throughout the MD simulations, the equation of motion was integrated with a time step of $0.001\sqrt{m\sigma^2/\varepsilon}$. Center of mass motion was removed from the simulation at a frequency of every 5000 steps.

We performed equilibrium MD simulations under the NVT constraints, i.e., the number of atoms, volume, and temperature are fixed at constant values. We first put the fluid atoms at evenly distributed lattice sites with an appropriate separation between the neighbors, determined from the fluid number density ρ. Then we add three layers of solid atoms arranged with face-centered-cubic structure both above and beneath the inserted fluid atoms. The fluid region's geometric size is $2L \times 2H \times 2W$ with $2H = 34.96\sigma$, where H denotes the position of the liquid-solid interface. The channel's periodicity along the x direction is set by $2L = 2H$. Channel's y direction periodicity is chosen to be $2W = 5.2\sigma$, for ensuring the eigenmodes' oscillations along the y direction is suppressed. Once the initial configuration was prepared, it was evolved for around 50 000 time steps in order to attain the equilibrium state. All the eigenmodes projections and correlation measurements discussed below were carried out at the equilibrium state. In what follows, unless explicitly stated, *reduced units will be used by default*.

B. Projected autocorrelation function of the eigenmodes

Using the continuum form of the HMs, projected unto the MD configurations, is an important initial step in our approach to obtain the HM's eigenvalues from MD as mentioned above in Sec. III.

The hydrodynamic eigenmodes' projected autocorrelation function $C_\beta(k_z, \Delta t)$ was measured for a particular eigenmode β with the input eigenwave vector k_z values ranging from 0.001 to 0.800 with an interval of 0.001. It is defined as

$$C_\beta(\Delta t) = \frac{\left\langle \left(\sum_i^N \vec{u}[\vec{r}_i(t_0)] \cdot \vec{v}_\beta[\vec{r}_i(t_0)]\right)\left(\sum_i^N \vec{u}[\vec{r}_i(t_0+\Delta t)] \cdot \vec{v}_\beta[\vec{r}_i(t_0+\Delta t)]\right)\right\rangle}{\left\langle \left(\sum_i^N \vec{u}[\vec{r}_i(t_0)] \cdot \vec{v}_\beta[\vec{r}_i(t_0)]\right)\left(\sum_i^N \vec{u}[\vec{r}_i(t_0)] \cdot \vec{v}_\beta[\vec{r}_i(t_0)]\right)\right\rangle}, \tag{10}$$

where the angular brackets denote ensemble averaging over t_0, $\vec{v}_n[\vec{r}_i(t)]$ denotes the βth hydrodynamic velocity eigenmodes value at position $\vec{r}_i(t)$, which is the coordinate vector of atom i at time t, $\vec{u}[\vec{r}_i(t)]$ denotes the MD velocity vector of ith atom at position $\vec{r}_i(t)$, and N is the total number of fluid atoms in the simulation domain. To ensure that the hydrodynamic statistical average is established and that the measurement is precise, we choose the time resolution $\Delta t = 0.02\sqrt{m\sigma^2/\varepsilon}$ to be 20 times larger than the integration time step. By measuring the normalized time correlation of a specific eigenmode β from MD, we are able to obtain the decay time $\tau = 1/\lambda$, which can be determined by the slope of the autocorrelation function.

C. Evaluating the diffusion constant from MD trajectories

We would like to evaluate an important parameter that is the result of equilibrium fluctuations—the diffusion constant—from MD atomic trajectories. We note that the diffusion constant can be evaluated by more than one approach, e.g., through the Green-Kubo relation [2] as the time integral of the velocity autocorrelation function. However, accuracy of this approach is poor, owing to the statistical fluctuations in the long time tail of the autocorrelation function. Here we use the ensemble-averaged atomic trajectories to calculate the diffusion constant by using the Einstein relation [2]:

$$\lim_{t\to\infty} \frac{\langle [x(t) - x(0)]^2 \rangle}{2t} = D. \tag{11}$$

By choosing an appropriately large-sized box as our monitoring window and limit the time interval to be small enough so that no atoms within the box would drift out, we plot the half the mean-squared distance versus the time interval Δt as shown in Fig. 3. Diffusion constant can be determined by evaluating the asymptotic slope as $t \to \infty$. This procedure yields $D = 0.20\sqrt{\varepsilon\sigma^2/m}$. This value can serve as the reference to be compared with that obtained from the fluctuation-dissipation theorem by using the HMs, shown in Sec. VI.

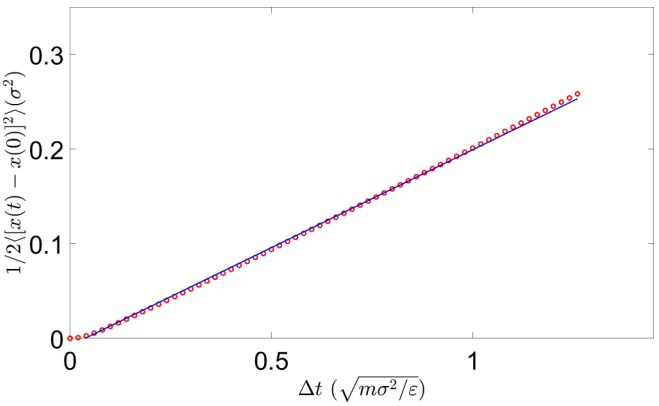

FIG. 3. A plot of the Einstein relation $\langle [x(t) - x(0)]^2 \rangle / 2 \sim t$, evaluated from atomic trajectories. Diffusion constant is determined by the asymptotic slope as $t \to \infty$. Here the blue line denotes the guide to the eye for the straight line section of the simulation data, and the red circle symbols denote the MD simulation data. Note that the initial few points in the simulated trajectory data do not follow the diffusive behavior, but rather show a ballistic behavior. From the slope of the straight-line portion, we obtain the value of the diffusion constant to be 0.20 ± 0.01, in units of $\sqrt{\varepsilon\sigma^2/m}$.

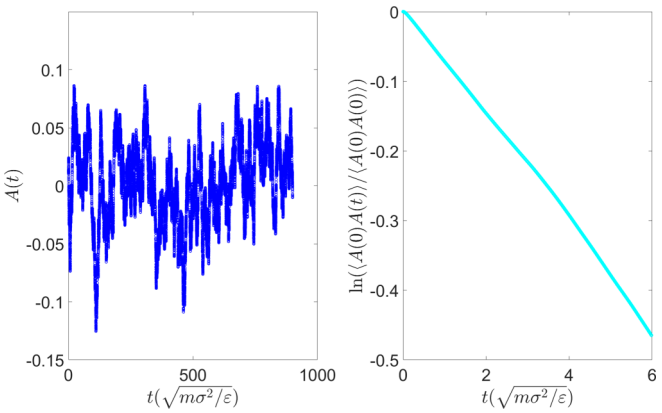

FIG. 4. (a) Instantaneous magnitude of the projection coefficient $A(t)$ for the eigenmode with $k_x = 0$, $k_z = 0.179/\sigma$. Each point is sampled from MD trajectories with a time interval $\Delta t = 0.02\sqrt{m\sigma^2/\varepsilon}$. (b) The logarithm of the autocorrelation function shows a good linear dependence with time t with a slope of $-0.074\sqrt{\varepsilon/m\sigma^2}$ when t is small, implying a decay time of $13.51\sqrt{m\sigma^2/\varepsilon}$. Deviation from linearity is seen when t becomes larger.

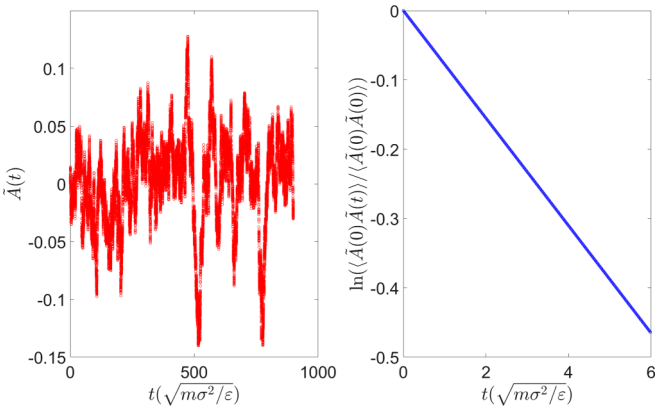

FIG. 5. (a) Time series $\widetilde{A}(t)$ with same time correlation behavior for the eigenmode $k_x = 0, k_z = 0.179/\sigma$. (b) The logarithm of the autocorrelation function $\langle \tilde{A}_k \tilde{A}_{k+m}\rangle / \langle \tilde{A}_k^2 \rangle$ shows exact linear dependence with t as expected, with a slope of -0.0776, implying a decay time of $12.9\sqrt{m\sigma^2/\varepsilon}$, which is 5% smaller than that obtained from MD.

V. GENERATION OF DISPLACEMENT VELOCITY TIME SERIES

Equation (10) gives the eigenmode-projected autocorrelation function $C_\beta(\Delta t)$ evaluated from MD trajectories. We would like to take a look at how the eigenmodes projection coefficient $A_\beta(t)$ evolves as a function of the instantaneous time t, and what its normalized autocorrelation function $C_\beta(t) = \frac{\langle A_\beta(0) A_\beta(t)\rangle}{\langle A_\beta^2(0)\rangle}$ looks like. $A_\beta(t)$ is defined as

$$A_\beta(t) = \frac{\sum_i^N \vec{u}[\vec{r}_i(t)] \cdot \vec{v}_\beta[\vec{r}_i(t)]}{\sum_i^N \vec{v}_\beta[\vec{r}_i(t)] \cdot \vec{v}_\beta[\vec{r}_i(t)]}. \tag{12}$$

From the completeness theorem, Eq. (9), we can express $\vec{u}[\vec{r}_i(t)] \cong \sum_\beta A_\beta(t)\vec{v}_\beta[\vec{r}_i(t)]$, where the approximation is in the replacement of the spatial integral in Eq. (9) by discrete summation. In Fig. 4(a) we plot the values of $A_\beta(t)$ at discretized time steps, i.e., $\{A(k\Delta t)\}$, where $k = 0, 1, 2, 3,...$ The effect of thermal fluctuations are easily seen. In Fig. 4(b) the logarithm of $C_\beta(t)$ is seen to present a good linear relation with time t, i.e., $C_\beta(t) = \exp(-\lambda_\beta t)$, even though at large t a slight deviation from linearity is seen.

We would like to generate both the thermal fluctuation time series and the corresponding autocorrelation function by using the same HM eigenfunction and eigenvalue, without using the MD. That can be useful sometimes as an alternative theoretical tool without invoking MD. In what follows we will ignore the subscript β.

Since A_k satisfies the constraints $\langle A_k\rangle = 0$ and $\langle A_k A_{k+m}\rangle = \Gamma^2 e^{-\lambda m \Delta t}$, where the angular brackets denote averaging over time steps k, it follows that by using the reparametrization we can recursively construct a correlated stochastic time series a_k:

$$a_0 = r_0, \quad a_k = e^{-\lambda\Delta t} a_{k-1} + \sqrt{1 - e^{-2\lambda\Delta t}}\, r_k. \tag{13}$$

Here $r_0, r_1, r_2, ...$ are independent variables that follows the Gaussian probability density function $\exp(-r^2/2)/\sqrt{2\pi}$. It can be easily verified that the time series a_k denotes a correlated Gaussian-distributed variable satisfying the correlation constraint $\langle a_k a_{k+m}\rangle = e^{-\lambda m\Delta t}$. That is, $\langle a_k\rangle = e^{-\lambda\Delta t}\langle a_{k-1}\rangle + \sqrt{1 - e^{-2\lambda\Delta t}}\langle r_k\rangle = 0$; and $\langle a_k^2\rangle = e^{-2\lambda\Delta t}\langle a_{k-1}^2\rangle + (1 - e^{-2\lambda\Delta t})\langle r_k^2\rangle = 1$. To build artificial thermal fluctuation time series $\widetilde{A}(t)$ with the same time correlation constraint of $A(t)$, we simply define $\tilde{A}_k = \Gamma a_k$ so that $\langle \tilde{A}_k\rangle = 0$ and $\langle \tilde{A}_k \tilde{A}_{k+m}\rangle = \Gamma^2 e^{-\lambda m\Delta t}$. In Fig. 5(a) we show the $\widetilde{A}(t)$ time series generated from the above recursive scheme. The autocorrelation is shown in Fig. 5(b). The decay time is about 5% lower than that shown in Fig. 4(b), but the time series resembles that obtained from MD, even though we do not expect them to be identical. It should be noted that the eigenmode used here has utilized the information about the position of the hydrodynamic boundary, i.e., the value of $h = H - \Delta$. In the following section we detail how this value of h is determined.

VI. HYDRODYNAMIC BOUNDARY AND THE SLIP LENGTH

In order to determine the position of the hydrodynamic boundary from the projected HMs in MD simulations, we would use the 2-tuple $\vec{k} = (k_x, k_z)$ characterization of the HMs, instead of the ordered eigenvalue index β. The basic idea is that for a given k_x, we input a discretized series of k_z values into the eigenfunctions, Eqs. (6) and (7). However, instead of trying to solve for the eigenvalues, which requires the knowledge about the position of the hydrodynamic boundary h as well as the value of the slip length, here we use MD to obtain both pieces of information. This process involves the following steps.

A. Projection of the form HM onto MD configurations

We directly project the HM eigenfunction with arbitrary values of k_z onto the MD simulations to obtain $C_{k_z}^{(k_x)}(\Delta t)$, i.e., Eq. (9), so as to obtain the inverse of its slope (i.e., the decay time τ) when plotted as a function of Δt.

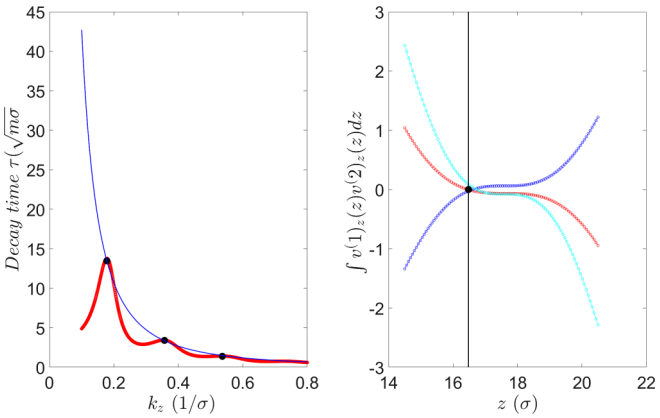

FIG. 6. (a) Decay time τ plotted as a function of k_z, discretized by intervals $\Delta k_z = 0.001/\sigma$ for the $k_x = 0$ case. Three black dots correspond to the peak points of the red curves, which theoretically predict the hydrodynamic modes' eigenwave vector k_z as well as its decay time. The upper blue curve corresponds to the relation $\tau k_z^2 = \rho/\eta$, where the viscosity $\eta = 1.95\sqrt{\varepsilon m}/\sigma^2$. The black dots denote the intersections of the blue curve with the red curve, from which the eigen-k_z values are picked out. (b) Hydrodynamic boundary position should satisfy the constraint of mutual orthogonality. Here the integral of three cross products are shown as a function of the upper integration limit. The three integrals of the cross products all vanishes in the vicinity of $h = 16.48\sigma$.

B. Determination of k_z and hence the eigenvalue of the HM

Since arbitrary values of k_z do not necessarily satisfy the boundary condition *that is implicit in the MD simulations,* we expect the decay time τ to be a maximum when the k_z value actually meets the boundary condition requirement in the MD simulations. In this manner we can easily identify the eigenvalues of the HMs, or the eigen-k_z values, directly from MD. For those values of k_z that do not meet the implicit MD boundary condition requirement, the decay time should be shorter since the discrepancy with the boundary condition necessarily invokes more dissipation owing to the incompatibility. This aspect can be seen from the variational derivation of the Navier boundary condition [15,16], which dictates minimum dissipation when the Navier boundary condition is satisfied. When supplemented by the HMs, the position of the hydrodynamic boundary becomes a parameter that can be (over-)determined from MD.

In Fig. 6(a) the red curve shows the decay time τ plotted as a function of k_z, discretized by interval $\Delta k_z = 0.001$ for the $k_x = 0$ case. It turns out that the $k_x = 0$ case is the simplest in terms of the determination of the hydrodynamic boundary position h. The reason is that for the $k_x \neq 0$ case, *a priori* knowledge of h is necessary in the calculation of $C_{k_z}^{(k_x)}(\Delta t)$. Therefore the strategy here is to first determine h from the $k_x = 0$ case, then to test the consistency with the $k_x \neq 0$ case. In Fig. 6(a) the blue curve denotes the relation $\tau k_z^2 = \rho/\eta$, with a viscosity value of $\eta = 1.95\sqrt{\varepsilon m}/\sigma^2$. The intersections of the blue curve with the red curve are marked by three black dots, which also correspond to the peaks of the decay time curve. In this manner the fluid viscosity is simultaneously determined.

TABLE I. Fluid hydrodynamics parameter values.

	Mode 1	Mode 2	Mode 3	Mode 4
k_z for MD	0.178	0.357	0.536	0.731
k_z for theory	0.178	0.357	0.537	0.720
$\Delta(\sigma)$		1.0 ± 0.1		
Slip length $l_s(\sigma)$		1.2 ± 0.1		
Viscosity ν $(\sqrt{\varepsilon m}/\sigma^2)$		1.9 ± 0.1		

C. Using the orthogonality relation to determine the HDB position and the slip length

To fix the location of the hydrodynamic boundary, we input the k_z values as indicated by the three black dots in Fig. 6(a) to the $k_x = 0$ HMs, which are just $\sin(k_z z)$. Three cross products can be formed from the three modes, denoted as 12, 13, and 23. The integration of these three cross products, starting at $z = 0$ upward, must vanish at the same hydrodynamic boundary since they have to be orthogonal to each other. By carrying out the integration as a function of z, we monitor the position of the first zero crossing. This is shown in Fig. 6(b), where the three cross products are shown to all cross zero at around $z = 16.48\sigma$. This value of z is denoted the hydrodynamic boundary position h. Since the molecular interface is located at $H = 17.48\sigma$, there is an offset of $\Delta = \sigma$ for the hydrodynamic boundary, which is inside the fluid domain. The reason for this offset is understandable, since in MD it is well known that there can be large density oscillation(s) in the vicinity of the fluid-solid interface [8].

It should be noted that once the position of the HB is determined, the value of the slip length is also known and can be determined from the HMs eigenfunctions by substituting the eigenvectors $k_z^{(n)}$ into the dispersion relationships, Eq. (6d) or (7d), as noted earlier.

The relevant parameter values shown in Fig. 6 are tabulated in Table I.

Next we check the consistency of the hydrodynamic boundary position with the $k_x = \pi/L$ (2D) HM projected onto the MD simulation results. In these modes we use the information of the hydrodynamic boundary position h obtained from Fig. 6. The purpose here is to check the consistency. Figure 7 gives the relation between decay time versus k_z. The blue curve is the same as that in Fig. 6. The three black dots indicate the positions of the analytical HM predictions, based on the hydrodynamic boundary information obtained from the $k_x = 0$ (see Fig. 6) modes. They correspond very well with the peaks of the decay time (red curve) obtained from MD simulations through the projection approach, as well as with the intersections of the blue curve with the red curve.

VII. FLUCTUATION-DISSIPATION THEOREM

As first pointed out by Onsager, the equilibrium fluctuations of a phase variable are governed by the same transport coefficients as the relaxation process to equilibrium of the same variable. Hence there is an inherent connection between fluctuations and the dissipative coefficient, which is made explicit by the fluctuation-dissipation theorem [2,11,25]. Under the linear response approximation [2], this theorem states that

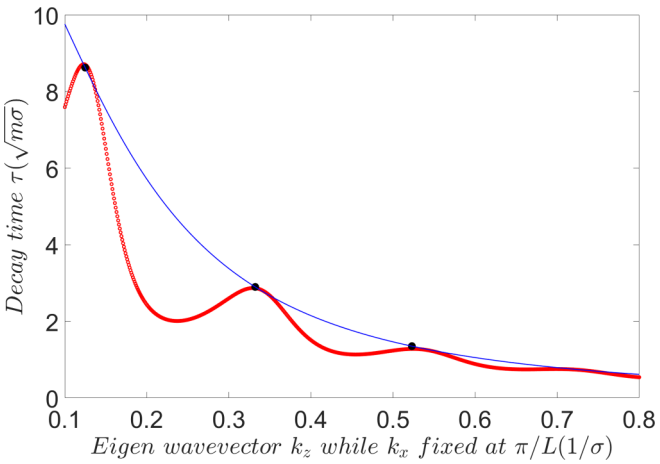

FIG. 7. Decay time τ plotted as a function of the eigenwave vector k_z discretized by intervals $\Delta k_z = 0.001$ for 2D hydrodynamic eigenmodes with $H = 17.48\sigma$ and k_x fixed at π/L. Three black dots correspond to the peak points of the red curves which theoretically predict the hydrodynamic modes eigenwave vector k_z and its decay time. According to eigenmodes property, $\tau(k_z^2 + k_x^2) = \rho/\nu$ should be a constant which is plotted as blue curves in the figure above. We can see that the blue curve passes through the black dots just as expected and we use the same hydrodynamic parameters here to show that they reflect the intrinsic solid-fluid intermolecular interactions.

the diffusion constant D can be expressed as a function of the time integral of the velocity autocorrelation function for a 2D fluid:

$$D = \frac{1}{2}\int_0^\infty \langle \vec{u}_i(0)\cdot\vec{u}_i(\tau)\rangle d\tau. \tag{14}$$

Here $\vec{u}_i$ denotes the 2D velocity vector of fluid atom i and the angular brackets represent the equilibrium ensemble average. We wish to express Eq. (14) from the perspective of HMs.

As seen from the previous section, at time t the molecular velocity can be expressed by superposing continuum hydrodynamic velocity eigenmodes. By substituting $A_\beta(t)$, Eq. (12), into Eq. (14) and invoking the completeness condition, we obtain

$$D = \frac{1}{2}\int_0^\infty \left\langle \sum_\beta \sum_\alpha A_\beta(0)A_\alpha(\tau)\vec{v}_\beta(0)\cdot\vec{v}_\alpha(\tau)\right\rangle d\tau. \tag{15}$$

Since each hydrodynamic eigenmode represents an independent degree of freedom, the cross-correlation $\langle A_\beta(0)A_\alpha(t)\rangle$ for $\beta \neq \alpha$ should be zero. Therefore,

$$\begin{aligned} D(x,z) &= \frac{1}{2}\int_0^\infty \left\langle \sum_\beta^{\beta_{\max}} A_\beta(0)A_\beta(\tau)|\vec{v}_\beta(x,z)|^2\right\rangle d\tau \\ &= \frac{1}{2}\int_0^\infty \sum_\beta^{\beta_{\max}} \langle A_\beta^2(0)\rangle\langle|\vec{v}_\beta(x,z)|^2\rangle e^{-\lambda_i\tau} d\tau \\ &= \frac{1}{2}\sum_\beta^{\beta_{\max}} \frac{1}{\lambda_\beta}\langle A_\beta^2(0)\rangle|\vec{v}_\beta(x,z)|^2. \end{aligned} \tag{16}$$

Here the summation is up to a maximum number of terms $\beta_{\max}$ so that the decay time $1/\lambda_\beta$ of the eigenmodes *falls within the diffusive regime*. We are reminded that too short a decay time is inconsistent with the relaxational behavior of the HMs, since it takes a few molecular collisions before the diffusive behavior is established and ballistic behavior obliterated.

The ensemble averaged $\langle A_\beta^2(0)\rangle = \Gamma_\beta^2 = (k_BT/\rho)/\int[v_{\beta,x}^2(x,z) + v_{\beta,z}^2(x,z)]dxdz$ can be determined directly from the equipartition theorem. The fluctuation-dissipation theorem is then given by the very simple expression:

$$\begin{aligned} D &= \frac{1}{A}\iint D(x.z)dxdz = \frac{1}{2}\frac{k_BT\beta_{\max}}{\rho A}\left[\frac{1}{\beta_{\max}}\sum_\beta^{\beta_{\max}}\frac{1}{\lambda_\beta}\right] \\ &= \frac{1}{2}\frac{k_BTM}{\rho}\left[\frac{1}{\beta_{\max}}\sum_\beta^{\beta_{\max}}\frac{1}{\lambda_\beta}\right] \end{aligned} \tag{17}$$

Here A denotes the area of the 2D sample, the quantity in the square brackets is the averaged decay time of the eigenmodes, up to the maximum $\beta_{\max}$, and $M = \lim_{A\to\infty}\beta_{\max}/A \cong 0.25/\sigma^2$ is shown in Appendix B to be a well-defined areal mode density.

By setting $1/\lambda_{\beta_{\max}} = 0.06\sqrt{m\sigma^2/\varepsilon}$ (the intercept of the straight line portion of the curve in Fig. 3), we obtain $\beta_{\max} \approx 4100$ and $D = 0.19\sqrt{\varepsilon\sigma^2/m}$, which is consistent with the diffusion constant value obtained from the slope of the straight line section in Fig. 3, i.e., $0.20\sqrt{\varepsilon\sigma^2/m}$, which has a standard error estimated to be around $0.01\sqrt{\varepsilon\sigma^2/m}$.

As far as we know, this is the first time that the fluctuation-dissipation theorem has been expressed in terms of the eigenvalues of the HMs. However, Eq. (17) should not be surprising since the FDT clearly involves a timescale, and that timescale turns out to be the averaged decay time of the hydrodynamic modes. The only constraint here is that the HM's decay time (inverse eigenvalue) should be within the diffusive regime so that the HM scheme is consistent with the basic assumptions of the FDT. In other words, while mathematically the HM's eigenvalue can approach infinity, physically there is an upper limit to the value of the eigenvalues for the validity of the FDT.

VIII. CONCLUSIONS AND OUTLOOK

We have formulated an alternative perspective on thermal fluctuations in a 2D channel that is based on HMs. It is shown that this approach can reproduce both the statistical time series of velocity fluctuations as that obtained from MD simulations, as well as their statistical properties. In particular, the FDT can be expressed in terms of the eigenvalues of the HMs. However, since the HMs inherently involves the boundary condition on the channel wall, it is shown that through the orthogonality condition of the HMs one can use MD simulations, in conjuction with the HMs, to accurately determine not only the location of the hydrodynamic boundary, but also the relevant slip length.

The HMs approach offers a complementary viewpoint on thermal fluctuations that can be useful when the boundary condition is involved. In looking ahead, we intend to explore

the effect of inhomogeneous modulation of the boundary condition along the channel walls, on the thermal fluctuations and their dynamic implications, such as the diffusion constant.

ACKNOWLEDGMENTS

P.S. wishes to acknowledge the support of Research Grants Council Grant No. 16303918 and a helpful discussion with T. Z. Qian at the initial stage of this work. X.H.D. acknowledges the helpful support of Han Wang, whose MD simulation code was used in this work.

APPENDIX A

Since it is well known that the eigenfunctions of a self-adjoint operator, in conjunction with the relevant boundary condition(s), form a complete and orthonormal set, here we give a simple proof that the HMs are indeed complete.

In order to reduce the number of constraints in Navier-Stokes equation, we introduce the scalar potential ϕ and rewrite the velocity field as

$$v_x = \frac{\partial \phi}{\partial z}, \quad v_z = -\frac{\partial \phi}{\partial x}, \tag{A1}$$

so that the incompressibility condition is automatically satisfied. Substituting Eq. (A1) into the Navier-Stokes equation we get

$$\nabla^2\nabla^2\phi + \lambda\nabla^2\phi = 0, \quad v_x(-L, z) = v_x(L, z), \quad v_z(-L, z) = v_z(L, z). \tag{A2}$$

In conjunction with the boundary conditions

$$l_s \frac{\partial v_x(x, \pm H)}{\partial z} \pm v_x(x, \pm H) = 0, \quad v_z(x, \pm H) = 0, \tag{A3}$$

periodic boundary conditions are applied at $x = \pm L$. Since slip length is uniform along the x direction, the scalar potential can be expressed as either

$$\phi(x, z) = \sum_{i=1}^{\infty} \widetilde{\phi}_i(z) \sin(m_i x) \tag{A4}$$

or

$$\phi(x, z) = \sum_{i=1}^{\infty} \widetilde{\phi}_i(z) \cos(m_i x), \tag{A5}$$

depending on whether the solution is symmetric or anti-symmetric modes we want to solve, where $m_i = i\pi/L, \quad i = 1, 2, 3, \ldots$.

By combining Eqs. (A1), (A4), or (A5) with Eq. (A2) we obtain

$$\frac{d^4\widetilde{\phi}_i}{dz^4} + p_1 \frac{d^2\widetilde{\phi}_i}{dz^2} + p_2\widetilde{\phi}_i = 0, \tag{A6}$$

where $p_1 = \lambda - 2m_i^2, \; p_2 = m_i^4 - \lambda m_i^2$.

Denote $\boldsymbol{O} = \frac{d^4}{dz^4} + p_1 \frac{d^2}{dz^2} + p_2$; we show that $\boldsymbol{O}$ is a self-adjoint operator, which means that

$$\begin{aligned} &\left\{u^*\left(\frac{d^4}{dz^4} + p_1\frac{d^2}{dz^2} + p_2\right)v - v\left[\left(\frac{d^4}{dz^4} + p_1\frac{d^2}{dz^2} + p_2\right)u^*\right]\right\}_{-h}^{h} \\ &= \left[u^*\frac{d^3v}{dz^3} - \frac{du^*}{dz}\frac{d^2v}{dz^2} + \frac{d^2u^*}{dz^2}\frac{dv}{dz} - v\frac{d^3u^*}{dz^3} + p_1\left(u^*\frac{dv}{dz} - v\frac{du^*}{dz}\right)\right]_{-h}^{h} \\ &= 0. \end{aligned} \tag{A7}$$

Here we have used the following equalities:

$$\begin{aligned} u^*\frac{d^4}{dz^4}v &= \frac{d}{dz}\left[u^*\frac{d^3}{dz^3}v\right] - \frac{d}{dz}\left[\frac{d}{dz}u^*\frac{d^2}{dz^2}v\right] \\ &\quad + \frac{d}{dz}\left[\frac{d^2}{dz^2}u^*\frac{d}{dz}v\right] - \frac{d}{dz}\left[v\frac{d^3}{dz^3}u^*\right] + v\frac{d^4}{dz^4}u^*, \\ u^*\frac{d^2}{dz^2}v &= \frac{d}{dz}\left[u^*\frac{d}{dz}v\right] - \frac{d}{dz}\left[v\frac{d^3}{dz^3}u^*\right] + v\frac{d^2}{dz^2}u^*. \end{aligned}$$

To show Eq. (A7) to be true, we use the Navier slip boundary condition at $z = \pm h$, which states that

$$\frac{d^2v}{dz^2} = \mp\frac{1}{l_s}\frac{dv}{dz}, \quad \frac{d^2u^*}{dz^2} = \mp\frac{1}{l_s}\frac{du^*}{dz}, \quad u^* = v = 0, \tag{A8}$$

and after simple reduction,

$$-\frac{du^*}{dz}\frac{d^2v}{dz^2} + \frac{d^2u^*}{dz^2}\frac{dv}{dz} = \pm\frac{1}{l_s}\frac{du^*}{dz}\frac{dv}{dz} \mp \frac{1}{l_s}\frac{du^*}{dz}\frac{dv}{dz} \equiv 0.$$

Hence $\boldsymbol{O}$ is a self-adjoint operator, and $\{\widetilde{\phi}_i\}$ forms a complete set.

Since $\{\sin(m_i x), \; m_i = i\pi/L, \; i = 1, 2, 3, \ldots\}$ and $\{\cos(m_i x), \; m_i = i\pi/L, \; i = 0, 1, 2, 3, \ldots\}$ together form a complete basis, denoted as $\{\kappa_i(x)\}$, and as HMs are the direct sum of the two complete basis $\{\widetilde{\phi}_i\}$ and $\{\kappa_i(x)\}$ in two independent subspaces, hence the HMs clearly form a complete and orthogonal basis.

APPENDIX B

For any given eigenwave vector k_x, there exists one and only one eigenwave vector $k_z^{(n)}$ in one periodicity. Therefore the total number of eigenmodes should be equal to the ratio of (k_x, k_z) domain area divided by the unit area $\Delta = (\pi/L) \times (\pi/H)$ occupied by each mode.

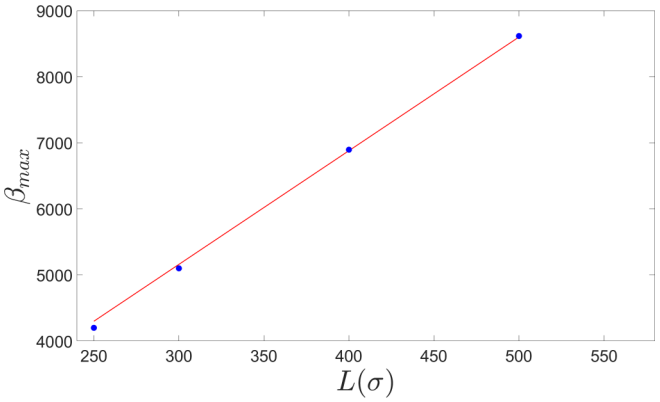

FIG. 8. The ratio of $\beta_{\max}$ and L is seen to be at a constant when L and H tend to infinity. This asymptotic value of the slope (red line) is $M \cong 0.263/\sigma^2$. Numerically evaluated values are indicated by blue dots. In our present case $M \cong 0.249/\sigma^2$ with $L = 250$.

We denote the minimum decay time as τ_0, then eigenvectors should obey the constraint:

$$\tau = \frac{R}{k_x^2 + k_z^2} \geqslant \tau_0, \quad k_x^2 + k_z^2 \leqslant \frac{R}{\tau_0},$$

where $k_x = \frac{n\pi}{L}$, $n = 0, 1, 2, 3, \ldots, N_x$, where N_x is the maximum integer satisfying $N_x = \lfloor \sqrt{\frac{R}{\tau_0}} \rfloor$. Hence for either the symmetric or the antisymmetric case,

$$\beta_{\max} \cong \lim_{H,L\to\infty} \frac{\pi \frac{R}{\tau_0} \times \frac{1}{4}}{\frac{\pi}{L} \times \frac{\pi}{H}}. \tag{B1}$$

The ratio of maximum $\beta_{\max}$ and $A = HL$ is therefore

$$M' = \lim_{H,L\to\infty} \frac{\beta_{\max}}{A} \cong \frac{\frac{R}{\tau_0}}{16\pi} \cong \frac{R}{16\pi\tau_0}.$$

Symmetric and antisymmetric modes have the same asymptotic property so

$$M = 2M' \cong \frac{R}{8\pi\tau_0}.$$

In Fig. 8, we plot the $\beta_{\max}$ as a function of channel's half-length L (with fixed H) numerically to illustrate the above linear dependency.

[1] K. Huang, *Statistical Mechanics*, 2nd ed. (Wiley, New York, 1987).
[2] M. Tuckerman, *Statistical Mechanics: Theory and Molecular Simulation* (Oxford University Press, Oxford, 2010).
[3] V. S. J. Craig, C. Neto, and D. R. M. Williams, Phys. Rev. Lett. **87**, 054504 (2001).
[4] S. Shen, G. Chen, R. M. Crone, and M. Anaya-Dufresne, Phys. Fluids **19**, 086101 (2007).
[5] J. S. Hansen, B. D. Todd, and P. J. Daivis, Phys. Rev. E **84**, 016313 (2011).
[6] J. P. Rothstein, Annu. Rev. Fluid Mech. **42**, 89 (2010).
[7] J. L. Barrat and L. Bocquet, Phys. Rev. Lett. **82**, 4671 (1999).
[8] S. Chen, H. Wang, T. Qian, and P. Sheng, Phys. Rev. E **92**, 043007 (2015).
[9] M. Allen and D. Tildesley, *Computer Simulation of Liquids* (Oxford University Press, Oxford, 1987).
[10] D. Frenkel and B. Smit, *Understanding Molecular Simulation from Algorithms to Applications,* 2nd ed. (Academic Press, San Diego, 2002).
[11] R. Kubo, Rep. Prog. Phys. **29**, 255 (1966).
[12] S. C. Bradford, Proc. Phys. Soc. **50**, 30 (1938).
[13] M. Stone and P. Goldbart, *Mathematics for Physics: A Guided Tour for Graduate Students* (Cambridge University Press, Cambridge, 2009).
[14] L. Landau and E. M. Lifshitz, *Fluid Mechanics*, 2nd ed. (Butterworth-Heinemann, London, 1987).
[15] T. Qian, X. P. Wang, and P. Sheng, J. Fluid Mech. **564**, 333 (2006).
[16] P. Joseph and P. Tabeling, Phys. Rev. E **71**, 035303(R) (2005).
[17] J. A. Martín, J. R. Meneghini, and V. Theofilis, Fluid Mech. Appl. **107**, 197 (2015).
[18] M. Sega, M. Sbragaglia, L. Biferale, and S. Succi, Soft Matter **9**, 8526 (2013).
[19] J. J. Thalakkottor and K. Mohseni, Phys. Rev. E **94**, 023113 (2016).
[20] E. Lauga, M. P. Brenner, and H. A. Stone, *Handbook of Experimental Fluid Dynamics* (Springer, New York, 2005).
[21] D. M. Huang, C. Sendner, D. Horinek, R. R. Netz, and L. Bocquet, Phys. Rev. Lett. **101**, 226101 (2008).
[22] M. S. Green, J. Chem. Phys. **22**, 398 (1954).
[23] F. A. Lindemann, Phys. Z. **11**, 609 (1910).
[24] G. J. Martyna and M. L. Klein, J. Chem. Phys. **97**, 2635 (1992).
[25] R. Kubo, J. Phys. Soc. Jpn. **12**, 570 (1957).